ELSEVIER

www.elsevier.nl/locate/jorganchem

Journal of Organometallic Chemistry 598 (2000) 182–186

Journal of Organometallic Chemistry

Note

Preparation of $[Et_2InSb(SiMe_3)_2]_3$; a trimeric single-source precursor to indium antimonide

Edward E. Foos [a], Richard J. Jouet [a], Richard L. Wells [a,*], Peter S. White [b]

[a] *Department of Chemistry, Paul M. Gross Chemical Laboratory, Duke University, Durham, NC 27708, USA*
[b] *Department of Chemistry, Venable Hall, University of North Carolina at Chapel Hill, Chapel Hill, NC 27514, USA*

Received 2 September 1999; received in revised form 29 October 1999

Abstract

The 1:1 mole ratio reaction of Et_2InCl with $Sb(SiMe_3)_3$ results in the formation of $[Et_2InSb(SiMe_3)_2]_3$ (**1**), a trimeric compound containing a six-membered indium–antimony ring. An X-ray crystal structure has been obtained for the compound substantiating the trimeric nature of **1** in the solid state, however variable-temperature ^{1}H-NMR studies show a dimer/trimer equilibrium for this species in solution. Preliminary thermolysis studies demonstrate its utility in the formation of nanocrystalline InSb.

Keywords: Indium antimonide; Precursor; Nanocrystalline; Trimer

1. Introduction

Recently, there has been a surge of interest in the preparation of organometallic compounds containing a direct Group 13 antimony bond. This interest stems from the fact that these compounds have traditionally been neglected during studies of other Group 13–Group 15 precursor systems, which are now prevalent in the literature [1]. As a result, a number of fully characterized compounds have been reported by ourselves [2] and others [3] which contain a direct bond between aluminum, gallium or indium and antimony, with the majority of the work thus far concentrated on gallium. Reports of indium–antimony compounds remain scarce, with $[t\text{-}Bu_2InSb(SiMe_3)_2]_2$ [2b], $(Me_3SiCH_2)_3In^{\bullet}Sb(SiMe_3)_3$ [2d], $[(Me_3SiCH_2)_2InSb(SiMe_3)_2]_2$ [2d], $[Me_2InSb(t\text{-}Bu)_2]_3$ [3d], $[(t\text{-}Bu_2Sb)(Cl)InSb(t\text{-}Bu)_2]_2$ [3e], and $[(Me_3SiCH_2)_2InSbMe_2]_3$ [3f] as the only examples of such compounds to be characterized in the solid state through X-ray crystallography. With the exception of $[Me_2InSb(t\text{-}Bu)_2]_3$ [3d], all of these compounds contain sterically demanding ligands bound to the indium atom. Our recent studies of gallium–antimony compounds incorporating ethyl groups on the Group 13 center [2a] have resulted in the isolation of several interesting compounds, and prompted us to examine similar reactions in the indium system. We report herein, as a result of these studies, the isolation, characterization and preliminary thermolysis of the trimeric compound $[Et_2InSb(SiMe_3)_2]_3$ (**1**).

2. Experimental

2.1. General considerations

All manipulations of air- and moisture-sensitive materials were performed in a Vacuum Atmospheres HE-493 Dri-Lab containing an argon atmosphere, or by standard Schlenk techniques. Hexane and toluene were distilled over sodium/potassium alloy under dry dinitrogen. Et_3In [4] and $Sb(SiMe_3)_3$ [5] were prepared from literature procedures. Et_2InCl was prepared from the 2:1 comproportionation reaction of Et_3In with $InCl_3$. $InCl_3$ was purchased from Strem Chemicals and used as

* Corresponding author.

0022-328X/00/$ - see front matter
PII: S0022-328X(99)00674-9

received. The integrity of starting materials, when applicable, was confirmed using ^{1}H-NMR spectroscopy. ^{1}H- and ^{13}C{^{1}H}-NMR spectra were recorded on a Varian Unity XL-400 spectrometer operating at 400 and 100.6 MHz, respectively. ^{1}H- and ^{13}C{^{1}H}-spectra were referenced to TMS using the residual protons or carbons of benzene-d_6 at δ 7.15 or δ 128.0, respectively. All NMR samples were prepared in 5-mm tubes, which were septum-sealed under argon. Powder X-ray diffraction (XRD) data were collected on a Phillips XRG-3000 diffractometer utilizing Cu–Kα radiation. Mass spectra were collected using a Jeol JMS-SX 102A spectrometer operating the EI+ mode at 20 eV. The melting point (uncorrected) was obtained with a Thomas-Hoover Unimelt apparatus, using capillaries that were flame-sealed under argon. IR spectra of volatile gases were acquired using a gas cell on a Bomem Michelson MB-100 FTIR spectrometer. Elemental analyses were performed by E+R Microanalytical Laboratory, Inc., Parsippany, NJ.

2.2. Preparation of $[Et_2InSb(SiMe_3)_2]_3$ (1)

Et_2InCl (0.208 g; 1.0 mmol) in 20 ml of hexane was added to a 250 ml round-bottomed flask equipped with a stir-bar and Teflon valve. A solution of $Sb(SiMe_3)_3$ (0.341 g; 1.0 mmol) dissolved in 20 ml hexane was then added via pipette at room temperature (r.t.), and an immediate color change to an orange–red mixture occurred. The red mixture was stirred for 12 h. The volatiles were removed in vacuo, and the dark solid was extracted with toluene. A small amount of hexane was added to the yellow solution, and storage at −30°C afforded thick, colorless needles of **1** (0.387 g, 88% yield). m.p. 132–140°C (dec. to a black liquid). Anal. Calc. for $C_{30}H_{84}In_3Sb_3Si_6$: C, 27.23; H, 6.4. Found: C, 27.36; H, 6.56%. ^{1}H-NMR: δ 0.52 (s, dimer, –$SiMe_3$), δ 0.56 (s, trimer, –$SiMe_3$), δ 0.82 (q, dimer, –CH_2CH_3), δ 1.19 (q, trimer, –CH_2CH_3), δ 1.44 (t, dimer, –CH_2CH_3), δ 1.62 (t, trimer, –CH_2CH_3). ^{13}C{^{1}H}-NMR: δ 5.79 (s, dimer, –$SiMe_3$), δ 5.94 (s, trimer, –$SiMe_3$), δ 10.16 (s, dimer/trimer, –CH_2CH_3), δ 14.21 (s, dimer, –CH_2CH_3), δ 14.75 (s, trimer, –CH_2CH_3). MS (m/e, ion): 853 ($[Et_2InSb(SiMe_3)_2]_2 - C_2H_5$)*; 795, ($[Et_2InSb(SiMe_3)_2]_2 - 3C_2H_5$)*; 651 ($[Et_2InSb(SiMe_3)_2]_2 - 3C_2H_5 - 2SiMe_3 + 2H$)*.

2.3. Variable-temperature ^{1}H-NMR study of 1

Approximately 0.017 g (0.013 mmol) of **1** was dissolved in 0.6 ml of benzene-d_6 and loaded into a 5 mm NMR tube, which was then flame sealed under reduced pressure. Spectra were taken at 25, 35, 40, 45, 50, 55, 60, and again at 25°C. Peaks corresponding to trimer and dimer were present in varying intensity ratios throughout the temperature range in which spectra were collected. The onset of thermal decomposition of **1**, characterized by the formation of several peaks from δ 0.28 to 0.03, was observed at 50°C. Upon cooling back to 25°C, it was apparent that the sample had undergone extensive decomposition during the experiment.

2.4. Thermolysis of $[Et_2InSb(SiMe_3)_2]_3$ (1)

Compound **1** (0.450 g, 1.02 mmol) was loaded into a sublimator which was attached to a liquid N_2 cold trap. The sample was heated under static vacuum to 400°C, where the temperature was maintained for 10 h. Significant sublimation of $[Et_2InSbSiMe_3)_2]_3$ was observed on the walls of the sublimator above the heat source. InSb was formed as a gray coating on the sides of the sublimator during thermolysis. This material was recovered (0.032 g, 13% yield) and its identity verified by comparison of the d-spacings and line intensities obtained by XRD analysis with those of InSb (JCPDS file 6-0208). Elemental In was also present in the sample and observed in the pattern (JCPDS file 5-0642). The approximate average particle size of 10 nm was calculated using the Scherrer equation. Condensable gases (0.72 mmol) were trapped during the decomposition, and identified as ethylene and $HSiMe_3$ through IR spectroscopy.

2.5. X-ray structural solution and refinement

A single crystal of **1** was mounted on a glass fiber with viscous oil under a stream of cold dinitrogen. X-ray intensity data were recorded at −135°C on a Bruker SMART CCD diffractometer utilizing graphite-monochromated Mo–Kα radiation ($\lambda = 0.71073$ Å) and the structure was solved by direct methods. Intensity data were collected to $2\theta = 50°$ resulting in 9789 unique reflections of which 5356 were considered observed and included in the subsequent computations. Full-matrix least-squares refinement with weights based upon counting statistics was performed. Hydrogen atoms were incorporated at their calculated positions using a riding model in the later iterations of refinement which converged at $R = 0.059$ ($R_w = 0.065$). The parameter to data ratio in the final cycle was 379 to 5356. A final difference Fourier synthesis revealed no unusual features. Crystallographic calculations were performed using the NRCVAX [6] suite of structure determination programs. For all structure-factor calculations, neutral atom scattering factors and their anomalous dispersion corrections were taken from Ref. [7].

3. Results and discussion

The 1:1 mole ratio reaction of Et_2InCl with $Sb(SiMe_3)_3$ results in the formation of **1** with concomi-

tant elimination of Me_3SiCl. Compound **1** is the third reported example of a solid state structurally characterized indium–antimony trimer, the others being the aforementioned $[Me_2InSb(t\text{-}Bu)_2]_3$ [3d] and $[(Me_3SiCH_2)_2InSbMe_2]_3$ [3f]. Each of these compounds contains a relatively undemanding alkyl group (methyl or ethyl), thus it seems reasonable that they all adopt similar trimeric conformations. Fig. 1 shows an ORTEP diagram of **1**, Table 1 lists crystallographic data for **1**, while Table 2 lists selected bond lengths and angles. The average indium–antimony bond length of 2.8732(15) Å found in **1** is the longest of the three reported trimeric compounds, with average indium–antimony bond lengths of 2.855(2) Å for $[Me_2InSb(t\text{-}Bu)_2]_3$ [3d] and 2.8615(6) Å for $[(Me_3SiCH_2)_2InSbMe_2]_3$ [3f]. The average endocyclic ring angles about indium and antimony in **1** of 104.38(5) and 125.13(5)°, respectively, compare favorably with the analogous average angles of 106.94(5) and 121.64(5)° in $[Me_2InSb(t\text{-}Bu)_2]_3$. The endocyclic ring angles in $[(Me_3SiCH_2)_2InSbMe_2]_3$ are significantly different when compared with these two compounds, with values of 95.94(2) and 132.83(2)°. This is attributable to the greater steric bulk of the Me_3SiCH_2 moieties bound to indium as well as the reduced steric bulk of the methyl groups on antimony. Significant variation can also be seen in the angles about the antimony atoms in **1**, which range from 119.09(5)° for In(1)–Sb(2)–In(2) to 129.69(5)° for In(2)–Sb(3)–In(3). Atoms In(1), Sb(1), In(2), and Sb(3) are very close to planar, with Sb(2) and In(3) located 1.1747(15) and 0.4908(17) Å, respectively, above the least squares plane. This indicates, in conjunction with the torsion angles (Table 2), that the core indium–antimony ring adopts a severely distorted twist-boat conformation (Fig. 2). Similar observations were made for $[Me_2InSb(t\text{-}Bu)_2]_3$.

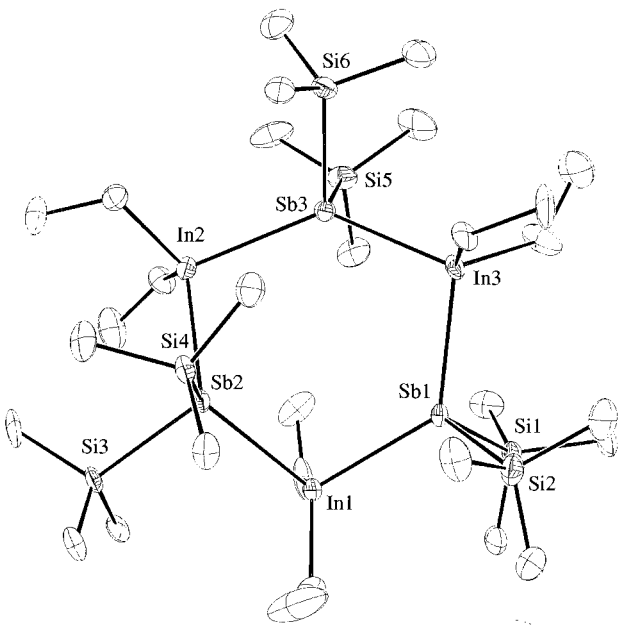

Fig. 1. ORTEP diagram (30% probability ellipsoids) showing the solid-state structure and atom numbering scheme for $[Et_2InSb(SiMe_3)_2]_3$ (**1**). Hydrogen atoms are omitted for clarity.

Table 1
Crystallographic data for $[Et_2InSb(SiMe_3)_2]_3$ (**1**)

Empirical formula	$C_{30}H_{84}In_3Sb_3Si_6$
Formula weight	1323.21
Space group	$P2_1/c$
Unit cell dimensions	
a (Å)	10.1899(4)
b (Å)	24.9740(10)
c (Å)	21.7632(9)
β (°)	93.605(1)
V (Å^3)	5527.4(4)
Z	4
Crystal color, habit	Colorless block
$D_{calc.}$ (g cm^3)	1.590
μ (Mo–K$_\alpha$) (mm^{-1})	2.82
Temperature (K)	173
No. of reflections measured	79 536
No. of unique reflections	9789
No. of observed reflections with $I>3.0\sigma(I)$	5356
Radiation	Mo–Kα ($\lambda = 0.71073$ Å)
$R(F)$ (%) [a]	5.9
$R(wF^2)$ (%) [a]	6.5

[a] Quantity minimized $= \Sigma[w(F_o-F_c)^2]/\Sigma[(wF_o)^2]^{1/2}$; $R = \Sigma\Delta/\Sigma(F_o)$, $\Delta = |(F_o-F_c)|$.

Like its gallium analogue [2a], **1** appears to exhibit a dynamic process in solution in that the r.t. ^{1}H-NMR spectrum contains two sets of the expected singlet–quartet–triplet peak pattern. This is indicative of an equilibrium exchange phenomenon and a variable-temperature ^{1}H-NMR study of **1** was conducted in an attempt to clarify this process. Due to the complexity of the ethyl region, analysis of the ratio of trimer to dimer was based on the integrated peak intensities of the antimony bound $SiMe_3$ moieties. Initially, at 25°C, there were two singlets present in this region at δ 0.52 and δ 0.57 in a ratio of 6.7:1. As the temperature was increased to 50°C this ratio fell to 1.9:1, however, at this temperature, the formation and growth of several peaks from δ 0.28–0.03 was observed indicating secondary elimination/decomposition events. As the temperature reached 60°C, the ratio of peak intensities fell to 1.5:1. Upon cooling of the sample back to 25°C, the ratio rose to 2.1:1. It is assumed that the sample then contained significantly less of the starting material **1** due to the aforementioned thermal decomposition processes. We are able to account for the smaller final ratio of trimer to dimer after cooling to 25°C because of the significant loss of starting material due to thermal decomposition, i.e. as the concentration of **1** decreases, the equilibrium favors the less-associated form. Because these peaks favor higher temperatures and lower con-

Table 2
Selected bond lengths (Å) and angles (°) for $[Et_2InSb(SiMe_3)_2]_3$ (**1**) with estimated standard deviations in parentheses

Bond lengths			
In(1)–Sb(1)	2.8741(15)	In(1)–Sb(2)	2.8583(15)
In(1)–C(71)	2.187(21)	In(1)–C(73)	2.231(17)
In(2)–Sb(2)	2.8707(15)	In(2)–Sb(3)	2.9113(15)
In(2)–C(81)	2.235(17)	In(2)–C(83)	2.179(16)
In(3)–Sb(1)	2.8241(15)	In(3)–Sb(3)	2.9010(16)
In(3)–C(91)	2.210(15)	In(3)–C(93)	2.237(18)
Sb(1)–Si(1)	2.575(5)	Sb(1)–Si(2)	2.624(5)
Sb(2)–Si(3)	2.580(4)	Sb(2)–Si(4)	2.597(5)
Sb(3)–Si(5)	2.630(5)	Sb(3)–Si(6)	2.538(5)
Bond angles			
Sb(1)–In(1)–Sb(2)	104.59(5)	Sb(1)–In(1)–C(71)	111.4(5)
Sb(1)–In(1)–C(73)	103.2(4)	Sb(2)–In(1)–C(71)	111.4(5)
Sb(2)–In(1)–C(73)	103.2(5)	C(71)–In(1)–C(73)	121.4(8)
Sb(2)–In(2)–Sb(3)	102.39(4)	Sb(2)–In(2)–C(81)	113.8(4)
Sb(2)–In(2)–C(83)	109.9(4)	Sb(3)–In(2)–C(81)	107.3(5)
Sb(3)–In(2)–C(83)	107.5(4)	C(81)–In(2)–C(83)	114.9(6)
Sb(1)–In(3)–Sb(3)	106.16(5)	Sb(1)–In(3)–C(91)	106.3(4)
Sb(1)–In(3)–C(93)	107.2(5)	Sb(3)–In(3)–C(91)	106.9(4)
Sb(3)–In(3)–C(93)	111.0(6)	C(91)–In(3)–C(93)	118.5(7)
In(1)–Sb(1)–In(3)	126.60(5)	In(1)–Sb(1)–Si(1)	102.34(11)
In(1)–Sb(1)–Si(2)	110.67(12)	In(3)–Sb(1)–Si(1)	107.81(11)
In(3)–Sb(1)–Si(2)	104.77(12)	Si(1)–Sb(1)–Si(2)	102.11(16)
In(1)–Sb(2)–In(2)	119.09(5)	In(1)–Sb(2)–Si(3)	101.39(11)
In(1)–Sb(2)–Si(4)	119.68(11)	In(2)–Sb(2)–Si(3)	111.28(12)
In(2)–Sb(2)–Si(4)	102.85(11)	Si(3)–Sb(2)–Si(4)	101.16(14)
In(2)–Sb(3)–In(3)	129.69(5)	In(2)–Sb(3)–Si(5)	103.64(13)
In(2)–Sb(3)–Si(6)	109.67(12)	In(3)–Sb(3)–Si(5)	110.34(12)
In(3)–Sb(3)–Si(6)	99.57(12)	Si(5)–Sb(3)–Si(6)	100.39(16)
Torsion angles			
Sb(2)–In(1)–Sb(1)–In(3)	−24.90(6)	Sb(3)–In(2)–Sb(2)–In(1)	−50.62(7)
Sb(3)–In(3)–Sb(1)–In(1)	−13.86(5)	Sb(1)–In(1)–Sb(2)–In(2)	+63.10(7)
Sb(2)–In(2)–Sb(3)–In(3)	+0.12(5)	Sb(1)–In(3)–Sb(3)–In(2)	+28.87(6)

centrations, the singlet occurring at δ 0.52, quartet at δ 0.82 and triplet at δ 1.44 can be assigned to the dimeric form of **1**. These peaks also lie upfield from those attributed to the trimeric form of **1**, consistent with observations made for $[Et_2GaSb(SiMe_3)_2]_2$ [2a].

It is interesting to note that three analogous antimony compounds with ethyl groups bound to the Group 13 metal have been prepared and examined utilizing X-ray crystallography: $[Et_2AlSb(SiMe_3)_2]_2$ [3c], $[Et_2GaSb(SiMe_3)_2]_2$ [2a], and **1**. Since these three compounds differ only by the Group 13 atom present in the monomeric unit, the effect of the metal in each is clearly demonstrated. For example, the aluminum compound has been fully characterized as a dimer in both the solution and solid phases. The sold state structure of the gallium analogue, $[Et_2GaSb(SiMe_3)_2]_2$, indicates it is dimeric in nature, yet it exhibits a well-behaved dimer/trimer equilibrium in solution with the predominant species in solution being the dimer [2a]. The solid state structure of **1** has been characterized as a trimer. Like the gallium analogue, **1** also exhibits a well-behaved dimer/trimer equilibrium in solution, however, in this case the species that predominates is the trimer.

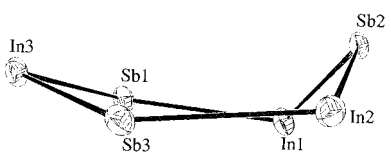

Fig. 2. ORTEP diagram (30% probability ellipsoids), side view, showing the distorted twist-boat conformation of $[Et_2InSb(SiMe_3)_2]_3$ (**1**). Silicon, carbon, and hydrogen atoms are omitted for clarity.

Preliminary investigations indicate that **1** can also serve as a single-source precursor to InSb. Thermolysis of this compound results in the formation of nanocrystalline InSb powder in low yield, which is contaminated with elemental indium. The low yield observed for this process is attributable to the significant sublimation of the precursor out of the hot zone of the apparatus during the course of the experiment. This sublimation is the result of the fact that **1** is extremely volatile. While detrimental to these studies, this volatility is a necessary requirement for any precursor that is to be used in a chemical vapor deposition process. Similar observations have been made for other ethyl-containing Group 13-antimony species [2a] and more detailed thermolysis studies on these compounds are currently being conducted.

4. Supplementary material

The structural data have been deposited with the Cambridge Crystallographic Data Centre: CCDC no. 136568. Copies of this information can be obtained from: The Director, CCDC, 12 Union Road, Cambridge, CB2 1EZ, UK (fax: +44-1223-336033; e-mail: deposit@ccdc.cam.ac.uk or www: http://www.ccdc.cam.ac.uk).

Acknowledgements

The authors thank the Office of Naval Research and the Lord Foundation of North Carolina for their financial support of this work.

References

[1] See the following and the references contained therein: (a) R.L. Wells, W.L. Gladfelter, J. Cluster Sci. 8 (1997) 217. (b) R.L. Wells, Coord. Chem. Rev. 112 (1992) 273. (c) A.H. Cowley, R.A. Jones, Angew. Chem. Int. Ed. Engl. 28 (1989) 1208.

[2] (a) E.E. Foos, R.J. Jouet, Wells, A.L. Rheingold, L.M. Liable-Sands, J. Organomet. Chem. 582 (1999) 45. (b) E.E. Foos, R.L. Wells, A.L. Rheingold, J. Cluster Sci. 10 (1999) 121. (c) R.L. Wells, E.E. Foos, P.S. White, A.L. Rheingold, L.M. Liable-Sands, Organometallics 16 (1997) 4771. (d) R.A. Baldwin, E.E. Foos, R.L. Wells, P.S. White, A.L. Rheingold, G.P.A. Yap, Organometallics 15 (1996) 5035.

[3] (a) S. Schulz, M. Nieger, Organometallics 18 (1999) 315. (b) S. Schulz, M. Nieger, J. Organomet. Chem. 570 (1998) 275. (c) S. Schulz, M. Nieger, Organometallics 17 (1998) 3398. (d) A.H. Cowley, R.A. Jones, C.M. Nunn, D.L. Westmoreland, Chem. Mater. 2 (1990) 221. (e) A.R. Barron, A.H. Cowley, R.A. Jones, C.M. Nunn, D.L. Westmoreland, Polyhedron 7 (1988) 77. (f) A.H. Cowley, R.A. Jones, Kidd, C.M. Nunn, D.L. Westmoreland, J. Organomet. Chem. 341 (1988) C1. (f) H.J. Breunig, M. Stanciu, R. Rösler, E. Lork, Z. Anorg. Allg. Chem. 624 (1998) 1965.
[4] D.F. Foster, D.J. Cole-Hamilton, Inorg. Synth. 31 (1997) 29.
[5] E. Amberger, G.R.W. Salazar, J. Organomet. Chem. 8 (1967) 111.
[6] E.J. Gabe, Y.L. Page, J.P. Charland, F.L. Lee, P.S. White, J. Appl. Crystallogr. 22 (1989) 384.
[7] International Tables for X-ray Crystallography, vol. IV, Kynoch Press, Birmingham, UK, 1974.